Theory of electric force microscopy in the parametric amplification regime

T. Ouisse,[1] M. Stark,[1,2] F. Rodrigues-Martins,[1] B. Bercu,[1] S. Huant,[1] and J. Chevrier[2,3]
[1]*Laboratoire de Spectrométrie Physique, Université Joseph Fourier, Grenoble 1 and CNRS (UMR C5588), 140, rue de la physique, B.P. 87, 38042, Saint-Martin d'Hères Cedex, France*
[2]*CNRS/LEPES, 25, avenue des Martyrs, 38042 Grenoble cedex 9, France*
[3]*European Synchrotron Radiation Facility (ESRF), BP220 38043 Grenoble cedex, France*
(Received 12 November 2004; revised manuscript received 13 January 2005; published 18 May 2005)

We propose to use a parametric amplification regime for small charge or potential difference detection in electric force microscopy. First we give a simple method to accurately estimate the instability domains of the oscillating system. Then we establish general and fully analytical expressions of the parametric amplification gain, and discuss the optimal parameter values which must be used for voltage or charge detection. We show that even in conventional Kelvin probe force microscopy the parametric effect should be taken into account.

DOI: 10.1103/PhysRevB.71.205404 PACS number(s): 68.37.Ps, 07.79.Lh, 73.90.+f

I. INTRODUCTION

Probing very small charge or electrostatic potential variations has become a key aspect in various fields of solid-state physics. For instance, such measurements are required for characterizing nanostructures or devices involving a small number of elementary charges,[1–7] detecting surface potential variations in a number of materials at the nanometer scale,[8–13] assessing dipole-dipole interactions[14] or studying electron transport in quantum structures.[15] For its ability to measure small variations of local properties, the atomic force microscope (AFM) has proven a powerful tool.[16] As a specialized technique, electric force microscopy (EFM), a derivate of dynamic force microscopy is actively investigated for its capacity to explore charge distributions in nanostructures. Typically, EFM is performed as a dynamic method.[2] A sinusoidal electric signal is applied to the investigated substrate at a frequency ω_{el} below the natural cantilever resonance ω_0, whereas a piezoelectric bimorph excites a metallized cantilever close to ω_0, so as to separate the frequency bands carrying the electrostatic and the mechanical signals, respectively. The electric force between the sample and the metallized tip results in a modulation of the amplitude oscillations at both ω_{el} and $2\omega_{el}$.

In this paper we propose to select adequate electric signal frequencies, so as to parametrically amplify the piezoelectric excitation, with the electric signal acting as a pump. In such a case, topography and electrical information cannot be acquired simultaneously, as usually achieved, but, e.g., in the lift mode technique. However, only one lock-in detection at a frequency around ω_0 is required. Parametric amplification has indeed already been observed in microactuators,[17] and has been used once in an AFM configuration in order to experimentally demonstrate thermomechanical noise squeezing.[18] Recently, it was explicitly demonstrated for mechanical excitation of the sample.[19] To the best of our knowledge no detailed theory of this phenomenon has been published in the case of an electrostatic force. Just to mention an already-existing technique, in the case of Kelvin probe force microscopy (KFM or KPFM) the electric signal is usually imposed close to ω_0. Although it is not ignored that there is a force component at $2\omega_{el}$, its effects are usually neglected, and only the ω_{el} component is considered.[8–13] However, the $2\omega_{el}$ component does lead to parametric amplification of the electric force component at ω_{el}. It is therefore necessary to ensure that this component does not appreciably modify the usual calculations. We will demonstrate in this paper that in many instances the parametric effect can drastically modify the magnitude of the oscillation usually expected in KFM.

To be able to use a parametric regime in EFM first requires a thorough understanding of its various effects, and it is our aim in this paper to provide such an understanding through a completely analytical approach, as well as some experimental evidence of the model validity. Then, we propose to use it for improving the sensitivity of charge detection or surface potential measurement. The article is structured as follows: Starting from the differential equation of the system, we describe a simple numerical method to calculate the instability domains of the cantilever oscillations, whatever is the form of the electric signal applied to the substrate, and to any degree of accuracy. The description of these instability domains leads to the extraction of conditions that are well adapted for charge or voltage detection. A fully analytical solution of the differential equation in the parametric regime with ω_{el} around $2\omega_0$ is given in the spirit of the treatment described by Rugar and Grütter some years ago,[18] yet with contrasting conclusions. The optimal setting of phase and voltage offset for voltage or charge detection are deduced as a function of the main physical parameters of the system. We show that if thermomechanical noise is not the prevailing noise source, the predicted sensitivity for charge detection can be increased by several orders of magnitude in comparison with the usual low frequency detection scheme. Although this paper is rather inclined toward treating the theoretical aspects of the problem, we report some experiments, conducted on a simple system, so as to illustrate the validity of our model and to show the relevance of our calculations. We also treat the case of an electric signal applied around ω_0, which induces as well parametric amplification, and which is actually used in KFM. Treating this case along with previous results will eventually permit us to discuss the impact of thermal noise.

II. DETERMINATION OF THE INSTABILITY DOMAINS OF THE CANTILEVER OSCILLATIONS

To find conditions suitable for charge detection the instability domains of the parametric system will be explored first. The general equation that governs the flexural cantilever vibrations is a fourth order one,[20] and in the high frequency range it is mandatory to consider all vibration modes.[20–22] Nevertheless, it is possible to model the cantilever as a harmonic oscillator driven by both an external driving force $F_p(t)$ resulting from a piezoelectric bimorph and an electric force $F_{\mathrm{el}}(t)$ exerted via the scanned substrate, as long as the investigated frequencies remain substantially lower than the second flexural vibration mode of the cantilever.[20,21] For a rectangular beam geometry the ratio between the frequencies of the two first flexural modes is 6.267,[20] and in order to exploit the parametric regime we are interested in frequencies up to $2\omega_0$. In our case the harmonic point-mass model is thus a reasonable approximation. The substrate is modeled as a metal plane above which a fixed charge Q_F can be located, at a given distance z_1 from the metal plane. The equation of the cantilever motion is

$$\frac{d^2z}{dt^2} + \frac{k_0}{m}z + \frac{\omega_0}{Q}\frac{dz}{dt} = \frac{F_p(t)}{m} + \frac{F_{\mathrm{el}}(z,t)}{m}, \tag{1}$$

with cantilever displacement $z(t)$, spring constant k_0, mass m and quality factor Q. The resonant frequency ω_0 is given by ${\omega_0}^2 = k_0/m$. In the general case the electrical force F_{el} does not necessarily behave as the force exerted between two perfect conductors,[10] most notably in the case of a low-doped semiconducting substrate,[23,24] and in some cases several mutual capacitances must be taken into account.[25] However, in most theoretical instances and in practice, the force is usually approximated as[26]

$$F_{\mathrm{el}} = \frac{1}{2}\frac{\partial C}{\partial z}(V + \Phi_{ST} + V_C)^2, \tag{2}$$

where Φ_{ST} denotes the work function difference between the metal plane and the metallized cantilever and C is the capacitance between the substrate and the cantilever. $V(t)$ represents the voltage applied to the substrate, while V_C is an equivalent voltage which results from the presence of the fixed charge (hence, as in the modeling of MOS capacitors, adding a fixed charge is equivalent to a flat-band voltage shift[26,27]). We will keep this approximation throughout, so as not to obscure the principles involved in the discussion by too great a bulk of numerical analysis. In the case of a plane-plane geometry, Eq. (2) is rigorous and becomes

$$F_{\mathrm{el}} = -\frac{\varepsilon S}{2}\left(\frac{V + \Phi_{ST} + \dfrac{Q_F z_1}{\varepsilon S}}{z + z_0}\right)^2, \tag{3}$$

where ε is the dielectric constant of the medium between the metal plate and the tip. The average distance z_0 accounts for the position of the conducting plane set on a defined potential. A development of the electrical force to first order in z turns Eq. (1) into

$$\frac{d^2z}{dt^2} + \left(\omega_0^2 - \frac{1}{m}\frac{\partial F_{\mathrm{el}}}{\partial z}\right)z + \frac{\omega_0}{Q}\frac{dz}{dt} = \frac{F_p(t)}{m} + \frac{F_{\mathrm{el}}(0,t)}{m}. \tag{4}$$

If the applied voltage V is an arbitrary periodic signal with pulsation ω and period T, the homogeneous equation of motion thus has the form

$$\frac{d^2z}{dt^2} + \left(\omega_0^2 - g(t)\right)z + \beta\frac{dz}{dt} = 0, \tag{5}$$

with $\beta = m\omega_0/Q$. Due to the periodicity of V, $g(t)$ is also a periodic function of the time, and is defined in (4). By changing the variable to $y = z\exp(\beta t/2)$ we obtain

$$\frac{d^2y}{dt^2} + \left(\omega_0^2 - \frac{\beta^2}{4} - g(t)\right)y = 0 \tag{6}$$

which can be further cast into the form

$$\frac{d^2y}{dt^2} + \theta(t)y = 0, \tag{7}$$

where $\theta(t)$ is periodic. This form is that of a Hill equation, and if the function $\theta(t)$ is given by a simple sine function, this equation further reduces to the well known Mathieu equation.[28]

In this parametric regime the solutions of the differential Eq. (7) are of the form $y = u(t)\exp(\mu t)$, where $u(t)$ is a periodic function of time.[28] Instability domains, corresponding to $\mu > 0$, can form in the frequency-amplitude plane of $\theta(t)$, under the form of instability tongues around the frequencies $\omega = 2\omega_0/n$, with an n integer.[28] Inside such instability domains, the oscillation amplitude is considerably increased with respect to the harmonic regime, and is indeed determined by the nonlinear terms neglected in Eq. (4). These instability domains have already been evidenced in the case of microactuators.[17]

Notably, it is also well known that the Mathieu equation is formally similar to a one-dimensional Schrödinger equation with a periodic sine potential (replace t by x). Indeed, determining the instability domains of Eq. (7) is formally identical to determine the energy band structure of an arbitrary one-dimensional periodic lattice. Moreover, it is of great interest to solve Eq. (7) for any arbitrary signal, as electric losses in the substrate changing the signal shape might have to be accounted for, or the use of electric pulses might be favorable. We are thus led to adapt a method originally proposed by Lee and Kalotas in the case of the Schrödinger equation.[29] We just outline its essential features and adapt them to the case discussed here in the Appendix. For each set of parameters, the stability condition (A12) is tested to map the instability domains in the corresponding planes. The examples given below will permit us to introduce the parametric conditions for charge detection.

In Fig. 1, condition (A12) has been used to map the instability domains in the voltage-frequency plane with the set of physical parameters listed in the figure caption. The black domains show the instability areas for a fixed charge equal to 150 elementary charges. In contrast, the superimposed grey domains are calculated for the same structure, free of any fixed charge. In both cases the electrical signal is sinusoidal.

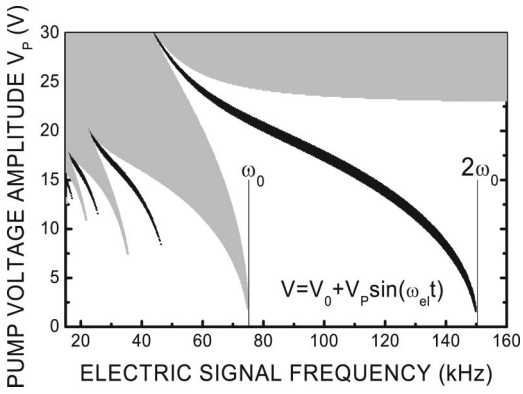

FIG. 1. Instability domains in the electric signal frequency-pump voltage plane, as calculated by applying the stability criterion of Eq. (A12) to a sinusoidal electric signal. Parameters: $S=2.25\times10^{-14}$ m^2, $m=10^{-11}$ kg, $k=2.23$ N/m, $Q=300$, *150* fixed elementary charges at $z_1=25$ nm, $z_0=50$ nm.

The grey domains which are only due to the alternative part $V_p \sin(\omega_{el}t)$ of the signal are almost the same in both cases, and superimposed. The highest frequency instability tongue due to V_P is obtained for $\omega_{el}=\omega_0$, since it gives a force component oscillating at $2\omega_0$ (see Eq. (3)). In contrast, adding a constant offset through the introduction of the fixed charge gives rise to a force component at ω_{el}, and a new instability tongue thus appears at $\omega_{el}=2\omega_0$. This is also quite clear in Fig. 2, for which the signal is now a sawtooth periodic voltage. For low voltage values the two first instability domains never exactly occur at ω_0 and $2\omega_0$, but rather take place at frequencies located below those values (see Figs. 1 and 2), because the resonance frequency of the cantilever is lowered by the constant part of the first order term in z of the electrical force. As detailed below, this is a favorable point for charge detection.

To enhance or lower drastically the natural oscillation amplitude of the cantilever A_0 through the action of a fixed

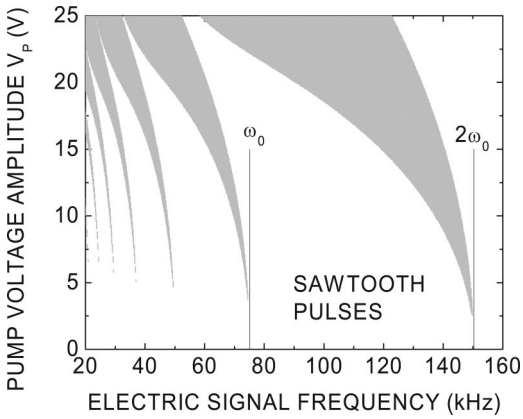

FIG. 2. Instability domains in the electric signal frequency-pump voltage plane, as calculated by applying the stability criterion of Eq. (A12) to a sawtooth electric signal with a linearly rising part and an abrupt falling part. Here V_P is defined as the amplitude of the sawtooth pulse and the base level is equal to *0* V. Parameters: $S=2.25\times10^{-14}$ m^2, $m=10^{-11}$ kg, $k=2.23$ N/m, $Q=300$, no fixed charges.

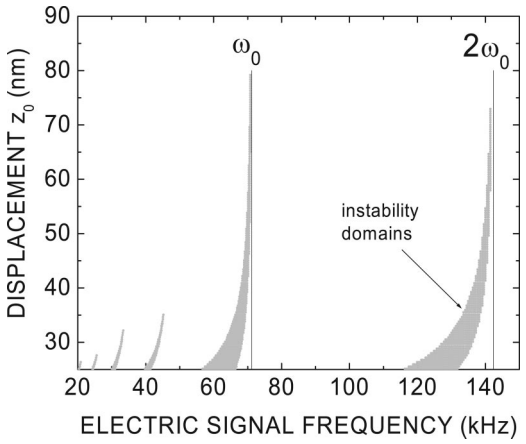

FIG. 3. Instability domains in the electrical signal frequency-displacement plane, as calculated by applying the stability criterion given by Eq. (A12) to a sinusoidal electric signal. Parameters: $S=6.25\times10^{-14}$ m^2, $m=10^{-11}$ kg, $k=2$ N/m, $Q=300$, 200 elementary charges at $z_1=20$ nm, pump voltage $V_P=5$ V.

charge or substrate voltage, the largest effect will clearly be obtained in the instability domains described above, since in such a case the oscillations are controlled by the nonlinear terms in Eq. (1). But these oscillations can indeed also become spontaneous and difficult to control if the tip is positioned close to the sample. Hence it is *a priori* preferable to stay out of the instability domain, but sufficiently close to it so as to remain in a parametric amplification regime, which is amenable to analytical calculations. This is for instance the case if one takes a sinusoidal signal with an electrical pulsation $\omega_{el}=2\omega_0$. As illustrated by Fig. 1 for $\omega_{el}=2\omega_0$, as V_P increases from zero to upper values, one progressively gets closer to the instability domain, up to a voltage above which one begins to go away from it. We thus expect an optimal amplification at a precise V_P value. A similar behavior is obtained in the frequency-position plane, as shown by Fig. 3. We will show that all quantities of interest can be accurately approached by simple analytical expressions.

III. CANTILEVER OSCILLATIONS WITH $\omega_{el}=2(\omega_0+\Delta\omega)$

A. Theory

First we derive the gain in amplification obtained in the case of a sinusoidal electrical excitation $V(t)=V_0+V_P\sin(2(\omega_0+\Delta\omega)t)$, with $\Delta\omega$ small against ω_0. Here, V_0 includes either an offset voltage, a work function difference, a fixed charge or a combination of the three terms. We will follow below an analysis very similar in spirit to that conducted by Rugar and Grütter in Ref. 18. As in Ref. 18, we introduce a new complex variable,

$$a=\frac{dz}{dt}+j\omega_1^* z, \tag{8}$$

$$a^*=\frac{dz}{dt}-j\omega_1 z, \tag{9}$$

with

$$\omega_1 = \omega_0\left(\sqrt{1-\frac{1}{4Q^2}}+\frac{j}{2Q}\right), \tag{10}$$

from which the inverse relations

$$z = \frac{a-a^*}{j(\omega_1+\omega_1^*)}, \tag{11}$$

$$\frac{dz}{dt} = \frac{\omega_1 a + \omega_1^* a^*}{\omega_1+\omega_1^*}, \tag{12}$$

can be obtained. Substituting (11) and (12) into Eq. (1) then yields

$$\frac{da}{dt} = j\omega_1 a + j\frac{k_p(t)}{m}\frac{a-a^*}{\omega_1+\omega_1^*} + \frac{F_{piezo}(t)}{m} + \frac{F_{\mathrm{el}}^0(t)}{m}, \tag{13}$$

where $k_p(t)$ is the modification of the spring constant induced by the electrical force and $F_{\mathrm{el}}{}^0(\mathrm{t})$ is the zeroth order term in z of the electrical force, depending on z_0. Equation (13) is similar to what was already obtained by Rugar and Grütter. However, we will not neglect any term in the first order expression of the electrical force as made in Ref. 18 (see our remark later). We make the additional hypothesis that the piezoelectric stimulation is ensured at a frequency half of the electrical excitation, so that parametric amplification acts on the piezoelectric oscillation,

$$F_p(t) = F_0\sin((\omega_0+\Delta\omega)t+\Phi). \tag{14}$$

Here we note an important difference with the treatment already given in Ref. 18: the authors assume that the frequency ω_0 involved in their equations is not the natural resonance frequency of the free cantilever, but rather the resonance frequency obtained with an offset voltage V_0 and pump voltage V_P *already applied* between the substrate and the cantilever. In other words, they implicitly include the constant part of $k_p(t)$ in the spring constant of the original system, and neglect the variation of the quality factor, which is also a function of V_0 and V_P. This is different from what we do in this article, since in their case, imposing $\omega_{\mathrm{el}}=2\omega_0$ means that the signal lies exactly below the instability tongue, so that as the pump voltage is increased, the gain continuously grows until spontaneous oscillations appear. They also make the hypothesis that the pump voltage remains negligible in front of the offset voltage, which is maintained constant (as achieved in their experiment). In our case, we seek a general solution for an arbitrary frequency around $2\omega_0$, and arbitrary voltages. Looking for a steady-state oscillation component of the form $a=a_0\exp(j(\omega_0+\Delta\omega)t)$, Eq. (25) leads to

$$j(\omega_1-\omega_0-\Delta\omega)a_0 - \frac{j\alpha}{m(\omega_1+\omega_1^*)}\left(\left(V_0^2+\frac{V_P^2}{2}\right)a_0 - \frac{V_0V_P}{j}a_0^*\right) + \frac{F_0}{2m}e^{j(\Phi+\pi/2)} = 0, \tag{15}$$

where

$$\alpha = \frac{1}{2}\frac{\partial^2 C}{\partial z^2}. \tag{16}$$

By noting that to first order in $1/Q, \omega_1{}^*+\omega_1 \approx 2\omega_0$ *and* $\omega_1-\omega_0 \approx j\omega_0/2Q$,[18] and defining

$$\beta_1 = \frac{\omega_0}{2Q}, \tag{17}$$

$$\beta_2 = \alpha\frac{V_0^2+\frac{V_P^2}{2}}{2m\omega_0}, \tag{18}$$

$$\beta_3 = \frac{\alpha V_0 V_P}{2m\omega_0}, \tag{19}$$

$$\beta_4 = \frac{F_0}{2m}, \tag{20}$$

we find after some calculation that a_0 can be expressed as

$$a_0 = \beta_4\frac{(\beta_1+\beta_3)\sin\Phi-(\beta_2+\Delta\omega)\cos\Phi - j((\beta_2+\Delta\omega)\sin\Phi+(\beta_1-\beta_3)\cos\Phi)}{\beta_1^2+(\beta_2+\Delta\omega)^2-\beta_3^2}, \tag{21}$$

so that the oscillation amplitude A at $\omega_0+\Delta\omega$ is

$$A = \frac{\beta_4}{\omega_0}\frac{\left(\beta_1^2+(\beta_2+\Delta\omega)^2+\beta_3^2-2\beta_3(\beta_1\cos 2\Phi+(\beta_2+\Delta\omega)\sin 2\Phi)\right)^{1/2}}{\beta_1^2+(\beta_2+\Delta\omega)^2-\beta_3^2} \tag{22}$$

(in (22) A is simply obtained from Eq. (21) by taking $A=|a_0|/\omega_0$). Equation (22) provides the ability to calculate analytically almost any quantity of interest in the parametric amplification condition $\omega_{\mathrm{el}}=2(\omega_0+\Delta\omega)$. Formula (22) is different from its counterpart derived in Ref. 18, since, as we will see below, A does not necessarily go to infinity when increasing V_P. Besides, for arbitrary V_P and V_0 values, the maximum amplitude is in general not obtained for a phase shift $\Phi=\pi/2$, as in Ref. 18. This can be seen in Figs. 4(a) and 4(b), where the amplitude of the oscillations has been plotted in the (V_0,V_P) plane for $\Phi=0$ and $\pi/2$, respectively, and $\Delta\omega=0$, the other parameters being analogous to that cho-

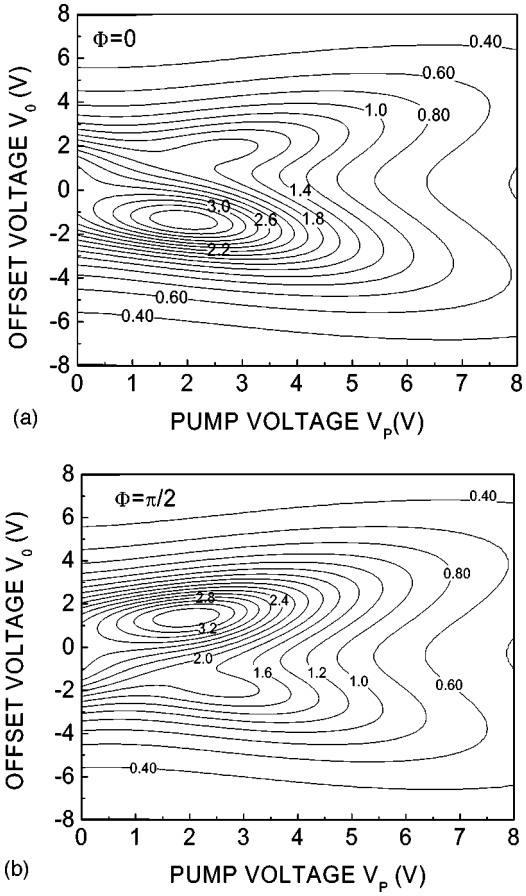

FIG. 4. Oscillation amplitude in the pump voltage V_P-offset voltage V_0 plane, as calculated from the analytical model of Sec. III. The isoamplitude line values are given in nm (from 0 to 4 nm with 0.2 nm steps). Parameters: $\omega_{el}=2\omega_0$, $\omega_{piezo}=\omega_0$, $S=2.25\times10^{-14}$ m^2, $z_0=50$ nm, $k=2.23$ N/m, $m=10^{-11}$ kg, $Q=300$, $F_{piezo}=2\times10^{-11}$ N, $f_0=75.16$ kHz (a) $\Phi=0$ and (b) $\Phi=\pi/2$.

sen in Fig. 1. In many areas the amplitude with $\Phi=0$ is larger than with $\Phi=\pi/2$.

From Eq. (22) it is straightforward to derive that if the condition

$$\frac{\partial^2 C}{\partial z^2} \geqslant \frac{2k}{Q|V_0 V_P|} \tag{23}$$

is fulfilled, i.e., if the tip position gets close enough to the sample, then the analytical gain goes to infinity if $\Delta\omega$ is comprised in a frequency interval given by the bottom and upper limits written below:

$$\Delta\omega_\infty^{\pm} = \frac{1}{2m\omega_0}\left(-\alpha\left(V_0^2+\frac{V_P^2}{2}\right) \pm \sqrt{\alpha^2 V_P^2 V_0^2 - \frac{k^2}{Q^2}}\right). \tag{24}$$

For a sinusoidal electrical excitation, those two limits analytically define the instability domains described in a more general way in the previous section. In the case of a plane capacitor condition (23) becomes

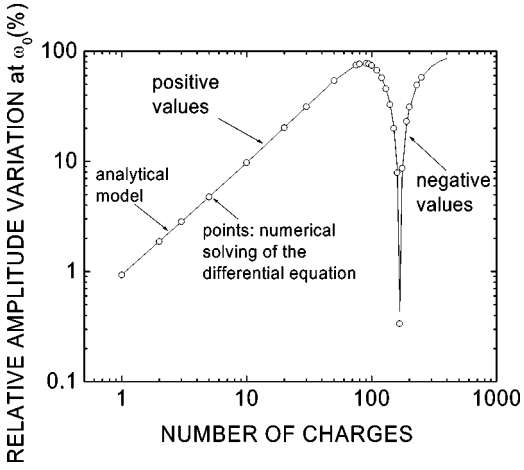

FIG. 5. Relative variation of the cantilever oscillation amplitude at ω_0 versus the number of elementary charges added to a plane at $z_1=25$ nm from the substrate plane. Points: numerical integration of Eq. (1) and solid line: analytical model. Calculation parameters: $\omega_{el}=2\omega_0$, $\omega_{piezo}=\omega_0$, $S=2.25\times10^{-14}$ m^2, $z_0=50$ nm, $V_P=V_{PC}=3.0567$ V, $\Phi=-3\pi/8$, $k=2.23$ N/m, $m=10^{-11}$ kg, $Q=300$, $F_{piezo}=2\times10^{-11}$ N, $f_0=75.16$ kHz.

$$z < \left(\frac{4\varepsilon SQ|V_0 V_P|}{k}\right)^{1/3}. \tag{25}$$

An important quantity is the maximum negative frequency shift $\Delta\omega_{\max}$ which can be imposed without entering into the instability domain during an approach-retract curve. Finding the value of α which renders $\Delta\omega_\infty^+$ minimum and recalculating the corresponding frequency shift leads to

$$\Delta\omega_{\max} = -\frac{\omega_0}{4Q}\sqrt{4\left(\frac{V_0}{V_P}\right)^2+\left(\frac{V_P}{V_0}\right)^2}. \tag{26}$$

Formulas (22), (23), (24), (25), and (26) give the opportunity to precisely select voltage, position and frequency conditions for which one can get as close as desired to the instability domain. The most favorable conditions for charge or potential detection are such that the gain is maximized without entering into the domain characterized by spontaneous oscillations. The closer to the instability domain one operates, the more sensitive is the method. A trade-off has thus to be chosen between gain and stability. For instance, a quite safe but somewhat restrictive measuring protocol might be to choose $\Delta\omega=0$, because the system never gets unstable and it even lends itself to a full analytical treatment: One must seek the condition for which a small variation in charge or potential (i.e., a change in V_0) induces the largest change in the oscillation amplitude, everything otherwise fixed. Hence one must solve $\partial A/\partial V_0=0$ (or $(\partial A/\partial V_0)/A=0$ if one is interested in maximizing a relative variation). But before determining this condition, we will first illustrate the precision of the analytical result through a comparison of formula (22) with a numerical integration of Eq. (1).

Equation (1) was numerically integrated in a number of realistic situations. The relative variation of A *versus* the number of elementary fixed charges added to the system is plotted in Fig. 5, with $\Delta\omega=0$, $z_0=50$ nm, $z_1=25$ nm, $V_0=0$

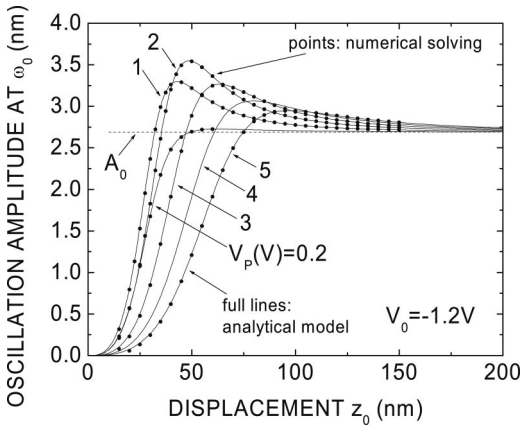

FIG. 6. Cantilever oscillation amplitude at ω_0 versus displacement z_0, for various pump voltage values. Points: Fourier component at ω_0 derived from a numerical integration of Eq. (1) and solid lines: analytical model. Parameters: $\omega_{el}=2\omega_0, \omega_{piezo}=\omega_0, S=2.25\times10^{-14}$ m^2, $V_0=-1.2$ V, $\Phi=0$, $k=2.23$ N/m, $m=10^{-11}$ kg, $Q=300$, $F_{piezo}=2\times10^{-11}$ N, $f_0=75.16$ kHz.

and $\Phi=-3\pi/8$ (as shown later on this Φ value indeed gives the highest variation for $V_0=0$). The agreement with the numerical calculations is excellent. Even for one elementary charge and a small surface capacitance, the variation in amplitude is around 1%. In Fig. 6 we simulated the variation of the amplitude with vertical displacement z_0. Once again the agreement between the numerical simulation and analytical result is excellent.

Figures 7(a) and 7(b) give the variation of the sensitivity $(\partial A/\partial V_0)/A$ in the (V_0, V_P) plane, for the same parameters as in Fig. 4, and for two different phase values. There are always some extrema of sensitivity in the plane. Although in the general case their determination requires to solve an algebric equation of order 7 in V_P, simplifying assumptions given the opportunity to find analytical expressions for all parameters. Below we will focus on the case $V_0=0$. Deriving Eq. (22) versus V_0 and making $V_0=0$ leads to the expression

$$\left.\frac{\partial A}{\partial V_0}\right|_{V_0=0} = -\frac{F_0\alpha V_P}{4m^2\omega_0^2}\frac{-\frac{\omega_0}{Q}\cos(2\Phi)+\frac{\alpha}{2m\omega_0}V_P^2\sin(2\Phi)}{\left(\frac{\omega_0^2}{Q^2}+\frac{\alpha^2}{4m^2\omega_0^2}V_P^4\right)^{3/2}}. \tag{27}$$

Equation (27) exhibits a maximum *versus* the phase if the relationship below is obeyed:

$$V_P^2 = -\frac{2k}{\alpha Q}\tan(2\Phi). \tag{28}$$

Here we note that Eq. (28) is also the condition for a maximum sensitivity, i.e., a maximum of $(\partial A/\partial V_0)/A$. Substituting V_P in Eq. (27) by the expression above, deriving versus Φ and finding the zeros of the resulting equation gives the conditions for which the phase and the pump voltage maximize $\partial A/\partial V_0$ at $V_0=0$:

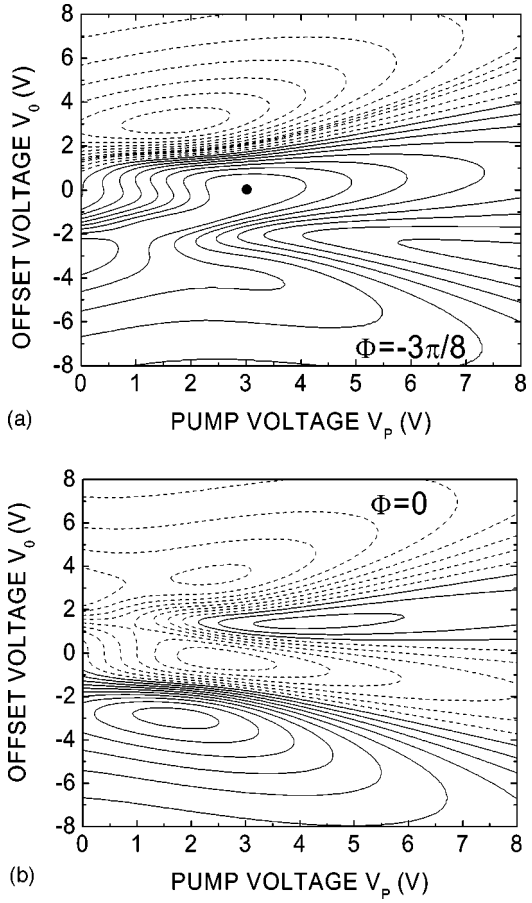

FIG. 7. Derivative of the oscillation amplitude divided by the amplitude in the offset voltage V_0-pump voltage V_P plane, as calculated from the analytical model of Sec. III. The solid lines are for positive values and the dashed lines are for negative values. Parameters: $\omega_{el}=2\omega_0, \omega_{piezo}=\omega_0, S=2.25\times10^{-14}$ m^2, $z_0=50$ nm, $k=2.23$ N/m, $m=10^{-11}$ kg, $Q=300$, $F_{piezo}=2\times10^{-11}$ N, $f_0=75.16$ kHz. (a) $\Phi=-3\pi/8$ and (b) $\Phi=0$. Taking $\Phi=-3\pi/8$ gives rise to a maximum on the line $V_0=0$ at $V_P=V_{PC2}$ (Eq. (32)), whose position is indicated by a black point.

$$\Phi_{C1} = \frac{\pi}{12} + n\frac{\pi}{2}, \tag{29}$$

$$V_{PC1} = \sqrt{\frac{2k}{\alpha Q\sqrt{3}}}, \tag{30}$$

with n integer. $\partial A/\partial V_0$ is then given by

$$\left.\frac{\partial A}{\partial V_0}\right|_{V_0=0}^{\max} = \frac{\pm F_0}{2}\left(\frac{Q}{k}\right)^{3/2}\sqrt{2\alpha\sqrt{3}}\left(1+\frac{1}{3}\right)^{-1/2}. \tag{31}$$

Quite similar conditions are obtained for maximizing $(\partial A/\partial V_0)/A$:

$$\Phi_{C2} = \frac{\pi}{8} + n\frac{\pi}{2}, \tag{32}$$

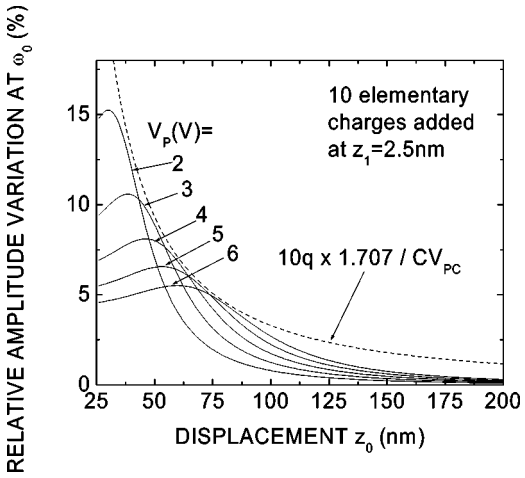

FIG. 8. Relative variation of the oscillation amplitude at ω_0 calculated for an approach-retract curve without charge and with ten added elementary charges. The dashed line represents the maximum variation which might be obtained by adjusting the pump voltage *versus* displacement z_0 according to Eq. (37). The two curves almost coincide when z_0 is such that $V_P = V_{PC2}$. Parameters: $\omega_{el} = 2\omega_0, \omega_{piezo} = \omega_0, S = 2.25 \times 10^{-14}$ m^2, $z_0 = 50$ nm, $z_1 = 25$ nm, $V_P = 2$, *3, 4, 5 and 6* V, $\Phi = \pi/8, k = 2.23$ N/m, $m = 10^{-11}$ kg, $Q = 300, F_{piezo} = 2 \times 10^{-11}$ N, $f_0 = 75.16$ kHz.

$$V_{PC2} = \sqrt{\frac{2k}{\alpha Q}}, \tag{33}$$

$$\frac{1}{A}\frac{\partial A}{\partial V_0}\bigg|^{\max}_{V_0=0} = \pm\sqrt{\frac{\alpha Q}{k}} = \pm\sqrt{\frac{Q}{2k}\frac{\partial^2 C}{\partial z^2}}. \tag{34}$$

For a given z_0 and $V_0 = 0$, Eq. (34) gives the highest possible sensitivity to a small charge or potential change which can be obtained with $\Delta\omega = 0$. It is worth noticing that a high sensitivity is not restricted to a narrow voltage range. As illustrated by Fig. 7(a), for $V_P = V_{PC2}$, the maximum sensitivity given by Eq. (34) is reduced by a factor of 2 for $V_0 = 1.315$ V and $V_0 = -1.639$ V, thus giving an acceptable operating window of almost 3 V. This would provide the provision necessary for operating the AFM without going out of the high sensitivity window. In the plane capacitor model, the maximum sensitivity varies as $z_0^{-3/2}$. Now suppose that a value of V_P has been fixed and $\Phi = \Phi_{C2}$. There is indeed a given value of z for which $(1/A)\partial A/\partial V_0$ is equal to expression (34). This is not the point where a maximum sensitivity is reached in the approach-retract curve (see Fig. 8 for an example), but interestingly enough, this maximum of sensitivity is located close to that value. Easy calculations show that with a fixed V_P and $\Phi = \Phi_{C2}$, the maximum sensitivity of the approach-retract curve is obtained for

$$\alpha_C = \frac{2(1+\sqrt{2})k}{QV_P^2} \tag{35}$$

and then is equal to

$$\frac{1}{A}\frac{\partial A}{\partial V_0}\bigg|^{\max}_{\substack{V_0=0 \\ \Phi=\Phi_{C2} \\ fixed\ V_p}} = \left(1+\frac{1}{\sqrt{2}}\right)\frac{1}{V_P} \approx \frac{1.707}{V_P}. \tag{36}$$

For a plane capacitor, the tip position for which this maximum is obtained is

$$z_0^C = \left(\frac{\varepsilon S Q V_P^2}{2k(1+\sqrt{2})}\right)^{1/3}. \tag{37}$$

A possible way to measure the equivalent voltage difference between two points or resulting from charge injection into the structure is to measure the maximum difference between the amplitude with and without charge in an approach-retract curve. The equivalent voltage difference ΔV_0^{eq} is simply given by

$$\Delta V_0^{eq}\big|_{\Phi=\pi/8}^{V_0=0} = \frac{V_P}{1.707}\mathrm{Max}\left(\frac{\Delta A}{A}\right), \tag{38}$$

where $\Delta A/A$ is the relative oscillation amplitude variation between the two approach-retract curves. The lower is V_P, the higher will be the maximum sensitivity but it will then be obtained for a closer distance between the tip and the sample, so that a trade-off must be chosen in order not to get influenced by additional forces and effects (see Fig. 8).

Finally we will illustrate through Fig. 9 the gain brought by the choice $\omega_{el} = 2\omega_0$ in comparison with the usual low frequency modulation of the cantilever oscillation which is obtained for $\omega_{el} < \omega_0$. We take $\omega_{el} = 2\pi \times 10$ kHz and all other parameters equal to the ones chosen in Fig. 5, and we add a single fixed charge to the system at $z_1 = 2.5$ nm. Figure 9 shows the power frequency spectrum of the cantilever oscillations, as calculated from a numerical integration of the equation of movement, Eq. (1). In Fig. 9 there is an eight-orders of magnitude difference between the line at *10* kHz and the line at ω_0. This is to be compared with the *1%* increase of the line at ω_0 in the case of parametric amplification (see Fig. 5). Thus in this example we predict that the latter method gives six orders of magnitude improvement in

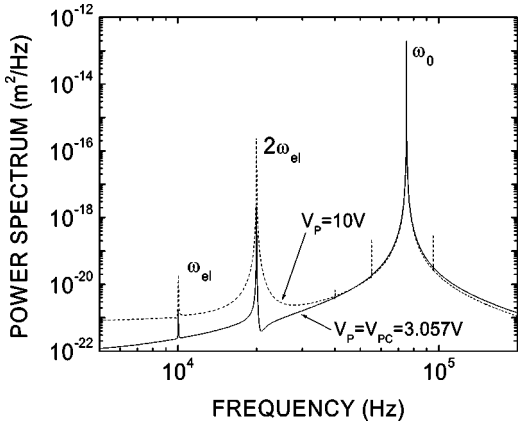

FIG. 9. Power frequency spectrum of the cantilever oscillations as calculated from a numerical integration of Eq. (1) with the same parameters as in Fig. 5, but $\omega_{el} = 2\pi \times 10$ kHz, $V_P = V_{PC2} = 3.056$ V (solid line) and $V_P = 10$ V (dotted line).

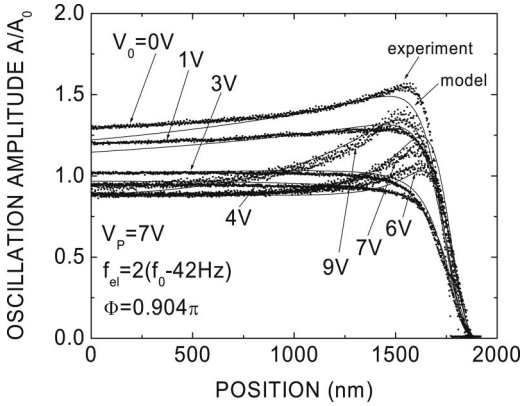

FIG. 10. Experimental approach-retract curves of an Au/Si plane in parametric amplification conditions, along with their fit with the analytical model. The fitting parameters are either experimentally extracted (ω_0, k, Q) or chosen to be very close to the values given by the tip supplier (cantilever dimensions). The electric signal frequency is slightly below $2\omega_0$. The fitting voltage values are all shifted by the same amount to take into account the contact potential difference between the tip and sample materials. The tip capacitance is modeled as a sphere and a cone, put in parallel with a plane capacitor corresponding to the cantilever area. $f_0 = 57.402$ kHz, $k = 4$ N/m, $Q = 200$, $f_{el} = 2(f_0 - 42\ \text{Hz})$, $f_{piezo} = f_0 - 42$ Hz, $\Phi = 0.904\pi$.

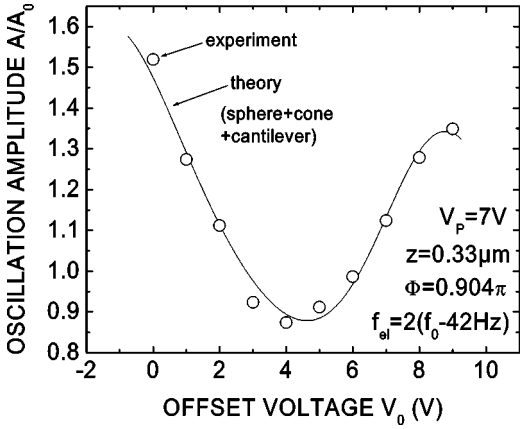

FIG. 11. Experimental variation of the oscillation amplitude as a function of offset voltage, with the tip positioned at 0.33 μm from the sample surface. The same parameters as in Fig. 10.

sensitivity in comparison with the former, if one takes into account all noise sources but thermal noise (to be treated in the last section). Increasing V_P so as to improve the sensitivity of the low frequency modulation does not substantially modify this ratio (case $V_P = 10$ V in Fig. 8). Besides, increasing F_0 or selecting a frequency in between $2\omega_0$ and $2(\omega_0 + \Delta\omega_{\max})$ could still greatly enhance the sensitivity without suffering from spontaneous oscillations.

B. Experiment

The preliminary data reported below are aimed at demonstrating the validity of our parametric amplification model. We use a homemade AFM head under construction, piloted by a Nanotec™ electronics system and equipped with Attocube™ micromotors. The piezoelectric signal is picked up by a homemade electronic circuit which exactly doubles the input signal frequency, with adjustable phase, offset and level outputs. The output signal is then applied to the sample, whereas the tip is connected to the electric ground. The approach-retract curves are obtained by using the Wsxm™ software. The optical detection is ensured by a Fabry-Perot cavity made up of the optic fiber extremity and the cantilever.[30] The cavity is adjusted through the application of a constant bias to a piezoelectric bimorph inserted in between the optic fiber head and the fixed setup.

Figure 10 shows typical experimental approach-retract curves, the sample being a flat gold surface, with an electric signal frequency chosen to lie slightly below $2\omega_0$. As can be seen in Fig. 10, the application of Eq. (34) with parameters either experimentally extracted (ω_0, Q, k) or chosen very close to the parameter values given by the tip supplier (cantilever dimensions, etc.) allows us to obtain very reasonable fits of the experimental curves, whatever is the offset voltage V_0. Here the capacitance is modeled as resulting from the parallel combination of a sphere+cone system (tip) and a plane capacitor (cantilever). For the tip we use the analytical electric force model proposed by Hudlet *et al.*[31] It is worth noticing that a perfect fit cannot be obtained for a number of reasons: for instance we do not take into account the 10 deg cantilever angle, and the sphere+cone model is only an approximation of the real geometry. Besides, the phase is also fitted because in practice there is a slight, constant dephasing between the electric signal applied to the piezoelectric bimorph which itself excites the cantilever, and the resulting cantilever oscillation. But even with such an approximate capacitance model, it is quite remarkable that the whole set of curves can be fitted with only one set of parameters. Close to the sample, the capacitance is dominated by the tip contribution, but far from it the cantilever influence prevails. Figure 11 gives the variation of the oscillation amplitude *versus* the offset voltage, now maintaining constant the position of the tip with respect to the sample. It also illustrates the nice agreement which can be obtained between the experiment and model. It is worth noticing that if the parametric effect was ignored, and just taking into account a "conventional" excitation close to $2\omega_0$, i.e., quite far from the resonance, the experimental approach-retract curves should be almost entirely determined by the piezoelectric excitation alone, and should remain almost unaffected by the sinusoidal electrical force. This is obviously not the case in Fig. 10.

As a last comment we note that we presented data obtained with a frequency just below $2\omega_0$, but when still reducing the electric signal frequency we did observe the nonlinear instability regime and all its characteristic features: frequency bifurcation with the apparition of a subharmonic component, strong and exponential increase of the oscillation amplitude, etc. This will be described elsewhere.

IV. CANTILEVER OSCILLATIONS WITH $\omega_{el} = (\omega_0 + \Delta\omega)$

Here we treat more briefly the case where the electric signal frequency is chosen to lie close to ω_0. First we note

that we deal with a very particular situation, since in this case both the excitation at ω_0 and the parametric amplification gain contain voltage terms. Second, it is worth noticing that this is not a mere academic problem, for this is the condition which is usually chosen in the case of KFM.[8–13,32] In this case we consider that both the piezoelectric excitation and the substrate voltage are applied at a frequency $\omega_0+\Delta\omega$. Defining

$$\gamma = \frac{1}{2}\frac{\partial C}{\partial z}, \tag{39}$$

$$\beta_5 = \frac{\gamma}{m} V_0 V_P, \tag{40}$$

$$\beta_6 = \frac{\alpha V_P^2}{8 m \omega_0}, \tag{41}$$

with calculations strictly similar to that conducted in Sec. III A, we find that the oscillation amplitude at $\omega_0+\Delta\omega$ is

$$A = \frac{\sqrt{\beta_5^2(\beta_1^2+(\beta_2-\beta_6+\Delta\omega)^2)+\beta_4^2(\beta_1^2+\beta_6^2+(\beta_2+\Delta\omega)^2-2\beta_6(\beta_2+\Delta\omega)\cos(2\Phi)+4\beta_1\beta_6\sin(2\Phi))+2\beta_4\beta_5(2\beta_1\beta_6\sin(\Phi)+((\beta_2+\Delta\omega-\beta_6)^2+\beta_1^2)\cos(\Phi))}}{\omega_0(\beta_1^2-\beta_6^2+(\beta_2+\Delta\omega)^2)}. \tag{42}$$

We will not study formula (42) with the same detail as its counterpart of Sec. III, but here we will rather discuss its implications on KFM, which is now an established technique. In general, the piezoelectric excitation is ensured at a frequency different from the electric one, the latter being around ω_0, so as to separate the two components, and the fact that the electric component at $2\omega_0$ parametrically amplifies the ω_0 component is not taken into account. From Eq. (42), making $\Delta\omega=0$ and $F_{piezo}=0$ leads to

$$A^{\Delta\omega=0}_{F_{piezo}=0} = \frac{\beta_5\sqrt{\beta_1^2+(\beta_2-\beta_6)^2}}{\omega_0(\beta_1^2-\beta_6^2+\beta_2^2)}. \tag{43}$$

From Eq. (43) one can easily find conditions for which the parametric effect is not at all negligible. However, for V_0 close to zero, the formula above simplifies to

$$A_{V_0\to 0} \cong 2|\gamma| V_0 V_P \frac{Q}{k}\frac{\sqrt{1+\left(\frac{\alpha Q V_P^2}{4k}\right)^2}}{1+3\left(\frac{\alpha Q V_P^2}{4k}\right)^2}. \tag{44}$$

If V_P itself is small, this further reduces to

$$A_{V_0,V_P\to 0} \cong -\frac{\partial C}{\partial z} V_0 V_P \frac{Q}{k}. \tag{45}$$

Formally the expression above is exactly the same as the one which is usually considered in KFM.[8] However, if V_P is large, or if z_0 gets small, Eq. (44) becomes

$$A_{V_0,z_0\to 0} \cong -\frac{8}{3}\frac{V_0}{V_P}\frac{\partial C}{\partial z}\left(\frac{\partial^2 C}{\partial z^2}\right)^{-1}, \tag{46}$$

which means that when the tip gets close enough to the sample the oscillation amplitude will start to decrease. In the plane capacitor case, the amplitude becomes proportional to the tip-sample distance $A\cong 4V_0 z_0/3V_P$. This is in complete contrast with the conventional approach, which predicts that the amplitude continuously increases as one gets closer to the sample, until the tip begins to tap the substrate or becomes sensitive to shorter range forces. On the other hand, in KFM the signal frequency is not necessarily equal to the natural frequency of the cantilever, but can be chosen so as to maximize the oscillation amplitude (i.e., at the resonance). What has been calculated here is an amplitude which is always calculated at the natural cantilever resonance frequency; without the parametric effect the amplitude at ω_0 should be lowered in comparison with Eq. (45), but here even for small V_P and V_0 values it is maintained constant by the parametric amplification. To find the best conditions for a Kelvin probe experiment we should use the frequency shift $\Delta\omega$ which makes the amplitude reaching a maximum. And in this case one recovers a situation similar to that discussed in the previous section. Depending on the parameter values and frequency, the parametric effect can considerably enhance the oscillation amplitude and one can even enter into the instability domain described in Sec. II. Without piezoelectric excitation at the same frequency the instability domain is reached if the inequality

$$V_P \geqslant V_{PC} = \sqrt{8\frac{k}{Q}\left(\frac{\partial^2 C}{\partial z^2}\right)^{-1}} \tag{47}$$

is verified and $\Delta\omega$ is comprised in the interval given by

$$\Delta\omega_\infty^{\pm} = \frac{1}{2m\omega_0}\left(-\alpha\left(V_0^2+\frac{V_P^2}{2}\right)\pm\sqrt{\frac{\alpha^2 V_P^4}{16}-\frac{k^2}{Q^2}}\right). \tag{48}$$

Close to such a domain the value of the amplification gain can become very high. Hence it is quite clear that in realistic systems the discrepancy between a simple-minded approach and the parametric solution can become extremely large. The experimental conditions should thus be carefully analyzed when the aim is to extract quantitative information from KFM, and to optimize the experimental conditions. An illustration of the quite substantial discrepancy which can arise between a conventional modeling and the parametric ap-

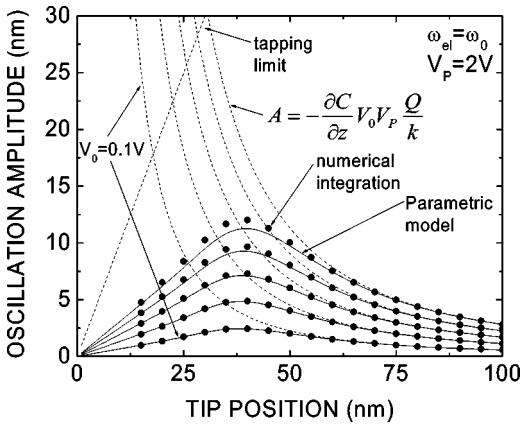

FIG. 12. Cantilever oscillation amplitude at ω_0 versus displacement z_0, for various offset voltage values. Points: Fourier component at ω_0 derived from a numerical integration of Eq. (1); solid lines: analytical parametric model, Eq. (42), and dashed lines: usual Kelvin probe approximation, Eq. (44). Parameters: $\omega_{el}=\omega_0, S=4\times10^{-14}$ m^2, $V_0=0$, *0.1, 0.2, 0.3, 0.4* and *0.5* V (from the lower to upper curves), $V_P=2$ V, $k=2.5$ N/m, $m=10^{-11}$ kg, $Q=200$.

proach is given by Fig. 12, which represents theoretical approach-retract curves calculated for a realistic system and using both models. From the numerical integration of the full differential equation, it is quite clear from Fig. 12 that the parametric approach is the correct one. Here we chose to use $\omega_{el}=\omega_0$, and Fig. 12 illustrates that close to the sample, i.e., in the most sensitive measurement domain, and well before the onset of tapping, the usual formula, Eq. (45), is considerably off the mark, and largely overestimates the oscillation amplitude. We note that the opposite situation (underestimated amplitude) could also be easily obtained, just by reducing the electric signal frequency slightly below ω_0, and closer to $\omega_0-\Delta\omega_\infty{}^+$. With incommensurate piezoelectric and electric frequencies, a good approximation of the resonance amplitude A_M can be found by making $\beta_4=0$ and taking the frequency which minimizes the denominator in Eq. (42). We obtain

$$A_M \cong 8\frac{\gamma}{\alpha}V_0V_P\frac{\sqrt{V_P^4+V_{PC}^4}}{V_{PC}^4-V_P^4}. \tag{49}$$

From (49), when V_P gets close to V_{PC}, the resonance amplitude largely exceeds the conventional one and is no longer proportional to V_P. This might explain the usual practice of operating with small V_P values, which here is justified by the concern for avoiding premature tapping due to the parametric effect. This might also explain some dependence of the measured potential on the driving amplitude, if this potential is not obtained by finding the value of V_0 which makes the amplitude vanish.

V. THERMOMECHANICAL NOISE

As already noted by Rugar and Grütter,[18] if one is interested in extracting data from the *excitation* which is parametrically amplified, there is no gain to expect from the usual thermomechanical noise limit, because both the useful excitation and the thermal fluctuations are amplified in the same way. However, in this section we wish to point out that the actual situation is somewhat more subtle, because in our case we do not want to extract information from an arbitrarily small excitation directly imposed upon the cantilever. We rather seek to obtain information which is contained in the gain, and not in the excitation to be amplified, and thus the latter can be made much larger than the thermomechanical noise. Here we briefly discuss this problem in a rather general way. Suppose that one wants to determine the value of a physical parameter ν which enters into the parametric force gradient, and not into the primary excitation. If A_0 is the amplitude of the piezoelectric excitation before amplification, much larger than the thermal noise amplitude A_B at $\omega_0+\Delta\omega$, and if G is the parametric gain, a small change $\Delta\nu$ in ν leads to an overall oscillation amplitude,

$$A \cong \left(G+\frac{\partial G}{\partial \nu}\Delta\nu\right)A_0 + GA_B. \tag{50}$$

The lowest detectable change in ν is thus

$$\Delta\nu_{\min} = \frac{G}{\dfrac{\partial G}{\partial \nu}}\frac{A_B}{A_0}. \tag{51}$$

From (51) one can enhance the sensitivity just by increasing the piezoelectric excitation, and the sensitivity is ultimately controlled by the maximum excitation value which can be safely chosen (for instance it cannot exceed the tip-sample distance), and by finding the conditions which maximize the relative variation of the gain with respect to the measured parameter, without entering into the spontaneous oscillation regime. To compare parametric amplification with other methods therefore requires us to compare expression (51) with the sensitivity given by the other technique, and *not* to calculate the smallest, preamplified excitation that exceeds the thermomechanical noise level. In the conventional case one must evaluate the minimum detectable amplitude when the force is now modulated at ω_0. The minimum detectable value ν_{min} is given by $F(\nu_{min})Q/k=A_B$, and must be compared to Eq. (51). In fact, in the regions where the amplification gain grows very rapidly, i.e., at the limit of the instability domains, it is in general possible to find conditions for which Eq. (51) is indeed better than the conventional limit. But it must be noted that on the one hand the system is not necessarily easy to control in those areas, and on the other hand the gain may be limited by the nonlinear terms in the differential equation. Hence in practice it may become rather difficult to select a measurement domain in which the parametric amplification gives better results than the conventional method with respect to thermal noise, and yet avoids the spontaneous oscillation regime. In the case of the electrical force the situation is particularly tricky, since the electric signal has components both at ω_{el} and $2\omega_{el}$, and thus even the case $\omega_{el}=\omega_0$ leads to parametric amplification. A detailed study of such a problem is beyond the scope of the present paper, and will be the subject of a future publication.

VI. CONCLUSION

Parametric amplification of a piezoelectric excitation by an electrical force may considerably enhance the sensitivity of AFM tip oscillations to small changes in charge or offset voltage between the tip and sample. In most interesting cases the amplification gain is amenable to accurate analytical calculations, and thus this method could lead to practical applications in EFM microscopy. Adapting this technique to charge detection is actually in progress in our laboratory. Besides, in this article we restricted ourselves to one Fourier component of the oscillation, but in most cases the spectrum is extremely rich and all other components may also include useful information, and can be analytically calculated. We also did not detail the nonlinear regime appearing in the instability domains, but we did observe it experimentally. Although more delicate to manage, the parametric effect could also be used in this regime. Eventually, we want to insist upon the fact that even if parametric amplification with $\omega_{\mathrm{el}}=2(\omega_0+\Delta\omega)$ is not used, this phenomenon is *not* an academic problem, but is very relevant in practice: the force resulting from an alternating electric signal intrinsically contains two frequencies, the value of the latter being exactly twice that of the former. Hence in EFM with sinusoidal electric excitation there is *always* parametric amplification, and its effects must be carefully analyzed, depending on the measurement conditions. In contrast to a widespread belief the ω component of the cantilever oscillation is not at all independent of the 2ω component of the electric force. We found that in KFM, the parametric effect prevails and determines the oscillation amplitude whenever the tip gets close to the sample. To the best of our knowledge this point seems to have been dismissed by previous authors in the AFM field. In the parametric amplification case, we also showed that calculating the thermomechanical noise limit is not as simple as with conventional techniques. This point will be the subject of a forthcoming publication.

ACKNOWLEDGMENTS

This work was financially supported by the program "Action concertée Nanosciences" ("EFM-subpico-Newton" project), and by CNRS, France. One of the authors (M.S.) gratefully acknowledges funding (Feodor-Lynen Fellowship) by the Alexander von Humboldt Foundation, Germany.

APPENDIX: DETERMINATION OF THE INSTABILITY DOMAINS

In this Appendix we summarize and adapt a method originally described by Lee and Kalotas to determine the band structure of one-dimensional solid lattices. Here we adapt it so as to determine the instability domains of Eq. (5). The method consists in calculating the exact solution of Eq. (7) for a suitably chosen periodic function which can be made arbitrarily close to the original $\theta(t)$ function, and then rigorously discuss the stability of this particular solution.

We break the function $\theta(t)$ over each period $t=\tau$ to $t=\tau+T$ into N constant segments of equal width $w=T/N$ and heights taken as the linearly interpolated mean $\theta_i=(\theta(\tau_i)+\theta(\tau_{i+1}))/2$ Eq. (7) in the ith segment becomes

$$\frac{d^2y}{dt^2}+\theta_i y=0. \tag{A1}$$

Defining $\gamma_i=\sqrt{-\theta_i}$, we express the solution in the ith segment as

$$y_i=a_i\cosh(\gamma_i(t-t_i))+\frac{b_i}{\gamma_i}\sinh(\gamma_i(t-t_i)). \tag{A2}$$

We define as in Ref. 15 the (2,2) unitary matrix

$$K(\gamma,w)=\begin{pmatrix}\cosh(\gamma w) & -\dfrac{\sinh(\gamma w)}{\gamma}\\ -\gamma\sinh(\gamma w) & \cosh(\gamma w)\end{pmatrix}. \tag{A3}$$

Imposing the continuity of the solution and its derivative at the boundary of each segment leads straightforwardly to the following condition:

$$\begin{pmatrix}a_1\\ b_1\end{pmatrix}=\Pi^{(1)}\begin{pmatrix}a_{N+1}\\ b_{N+1}\end{pmatrix}, \tag{A4}$$

where $\Pi^{(1)}$ stands for the product of the K matrices:

$$\Pi^{(1)}=\prod_{n=1}^{N}K(\gamma_n,w). \tag{A5}$$

Since the solutions of Eq. (6) are of the form $y=u(t)\exp(\mu t)$ with $u(t)$ periodic, the solutions $z(t)$ of Eq. (5) are such that

$$z(t+T)=z(t)e^{(\mu-\beta/2)T}. \tag{A6}$$

Hence, for z not to grow exponentially one must fulfill the condition

$$\left|e^{\mu T}\right|<e^{\beta T/2}, \tag{A7}$$

which restated in terms of the function y gives

$$y(t+T)=\lambda y(t)e^{\beta T/2}, \tag{A8}$$

where λ is a complex factor such that $|\lambda|\leqslant 1$. Rewriting Eq. (A6) in terms of the coefficients a_i and b_i, and taking also Eq. (A4) into account, one arrives at the linear equation system

$$\left(\Pi^{(1)}-\frac{e^{-\beta T/2}}{\lambda}I\right)\begin{pmatrix}a_1\\ b_1\end{pmatrix}=0, \tag{A9}$$

where I is the identity matrix. This system admits nontrivial solutions only if

$$\det\left(\Pi^{(1)}-\frac{e^{-\beta T/2}}{\lambda}I\right)=0. \tag{A10}$$

Defining Tr as the trace of the K-matrices product, and taking into account the unitarity of the K matrices, we arrive at the stability condition

$$\left|\mathrm{Tr}\pm\sqrt{\mathrm{Tr}^2-4}\right|<2e^{\beta T/2}, \tag{A11}$$

which can easily be turned into

$$|\mathrm{Tr}| < 2\cosh\left(\frac{\beta T}{2}\right). \tag{A12}$$

Verifying the stability condition (A12) provides the ability to determine the instability domains for any kind of electric signal. It is trivial to numerically implement this method, and the accuracy of the calculation only depends upon the precision chosen for segmenting the voltage over one period.

[1] B. D. Terris, J. E. Stern, D. Rugar, and H. J. Mamin, Phys. Rev. Lett. **63**, 2669 (1989).
[2] B. D. Terris, J. E. Stern, D. Rugar, and H. J. Mamin, J. Vac. Sci. Technol. A **8**, 374 (1989).
[3] T. D. Kraus and L. E. Brus, Phys. Rev. Lett. **83**, 4840 (1999)
[4] M. A. Salem, H. Mizuta, and S. Oda, Appl. Phys. Lett. **85**, 3262 (2004).
[5] D. M. Schaadt, E. T. Yu, S. Sankar, and A. E. Berkowitz, Appl. Phys. Lett. **74**, 472 (1999).
[6] C. Guillemot, P. Budau, J. Chevrier, F. Marchi, F. Comin, C. Alandi, F. Bertin, N. Buffet, Ch. Wyon, and P. Mur, Europhys. Lett. **59**, 566 (2002).
[7] T. Mélin, D. Deresmes, and D. Stiévenard, Appl. Phys. Lett. **81**, 5054 (2002).
[8] Y. Martin, D. W. Abraham, and H. Kumar Wickramasinghe, Appl. Phys. Lett. **52**, 1103 (1988).
[9] M. Nonnenmacher, M. P. O'Boyle, and H. K. Wickramasinghe, Appl. Phys. Lett. **58**, 2921 (1991).
[10] K. L. Sorokina and A. L. Tolstikhina, Crystallogr. Rep. **49**, 541 (2004).
[11] K. Okamoto, K. Yoshimoto, Y. Sugawara, and S. Morita, Appl. Surf. Sci. **210**, 128 (2003).
[12] S. Sadewasser, Th. Glatzel, R. Shikler, Y. Rosenwaks, and M. Ch. Lux-Steiner, Appl. Surf. Sci. **210**, 32 (2003).
[13] Th. Glatzel, S. Sadewasser, and M. Ch. Lux-Steiner, Appl. Surf. Sci. **210**, 84 (2003).
[14] T. Mélin, H. Diesinger, D. Deresmes, and D. Stiévenard, Phys. Rev. Lett. **92**, 166101 (2004).
[15] K. L. McCormick, M. T. Woodside, M. Huang, M. Wu, P. L. McEuen, C. Duruoz, and J. S. Harris, Jr., Phys. Rev. B **59**, 4654 (1999).
[16] F. J. Giessibl, Rev. Mod. Phys. **75**, 949 (2003).
[17] M. Napoli, B. Bamie, and K. Turner, *Proceedings of the American Control Conference*, 2003, p. 3732.
[18] D. Rugar and P. Grütter, Phys. Rev. Lett. **67**, 699 (1991).
[19] S. Patil and C. V. Dharmadhikari, Appl. Surf. Sci. **217**, 7 (2003).
[20] U. Rabe, K. Janser, and W. Arnold, Rev. Sci. Instrum. **67**, 3281 (1996).
[21] J. A. Turner, S. Hirsekorn, U. Rabe, and W. Arnold, J. Appl. Phys. **82**, 966 (1997).
[22] R. Stark, G. Schitter, M. Stark, R. Guckenberger, and A. Stemmer, Phys. Rev. B **69**, 085412 (2004).
[23] S. Hudlet, M. Saint-Jean, B. Roulet, J. Berger, and C. Guthmann, J. Appl. Phys. **77**, 3308 (1995).
[24] B. M. Law and F. Rieutord, Phys. Rev. B **66**, 035402 (2002).
[25] H. O. Jacobs, P. Leuchtmann, O. J. Homan, and A. Stemmer, J. Appl. Phys. **84**, 1168 (1998).
[26] J. Polesel-Maris, A. Piednoir, T. Zambelli, X. Bouju, and S. Gauthier, Nanotechnology **15**, S24 (2004).
[27] J. R. Brews, *MOS Physics and Technology* (Wiley, New York, 1982).
[28] N. W. McLachlan, *Theory and Applications of Mathieu Functions* (Oxford University Press, Oxford, 1951).
[29] A. R. Lee and T. M. Kalotas, Phys. Scr. **44**, 313 (1991).
[30] M. Vogel, B. Stein, H. Pettersson, and K. Karrai, Appl. Phys. Lett. **78**, 2592 (2001).
[31] S. Hudlet, M. Saint Jean, C. Guthmann, and J. Berger, Eur. Phys. J. B **2**, 5 (1998).
[32] P. Girard, Nanotechnology **12**, 485 (2001).